International Journal of GEOMATE, Sept., 2021, Vol.21, Issue 85, pp.137-144
ISSN: 2186-2982 (P), 2186-2990 (O), Japan, DOI: https://doi.org/10.21660/2021.85.j2085
Geotechnique, Construction Materials and Environment

PERFORMANCE OF SQUARE REINFORCED CONCRETE COLUMNS CONFINED WITH INNOVATIVE CONFINING SYSTEM UNDER AXIAL COMPRESSION

Soerjandani Priantoro Machmoed[1,2], Tavio[2]* and I Gusti Putu Raka[2]

[1]Department of Civil Engineering, Universitas Wijaya Kusuma Surabaya, Indonesia;
[2]Department of Civil Engineering, Institut Teknologi Sepuluh Nopember, Surabaya, Indonesia

*Corresponding Author, Received: 15 Jan. 2021, Revised: 01 Aug. 2021, Accepted: 26 Aug. 2021

ABSTRACT: Several structural failures occur in the column due to the lack of confinement. The circular column is not popular for regular buildings. The use of circular spiral is only familiar to the circular column. Many design engineers use square columns with hoops and cross ties as confinement. As far as the authors' knowledge, there was only a study carried out on square columns with circular spirals as confinement. For this reason, the authors propose and introduce a new type of innovative confinement system for square columns using square spirals as confinement and a combination thereof, which has never been carried out in the previous studies. No code's provision is also applicable to this type of confinement. This research was conducted to investigate the performance of each of these new confinement systems as a promising option in the future instead of the traditional confinement. To achieve the objective of the research, a two-phase study was conducted. The first phase was to analyze the potential, design, formation, and assembly of the new confinement system consisting of a combination of square and circular spirals (SPIL), a combination of octagonal and square spirals (SS8I), an interlocking among square spirals (SPIP), and a plain concrete specimen (PC) as a benchmark. The second phase was an experimental program that involves a mix-design of the concrete, preparation of the column specimens with various confinement systems, and the compression tests of the column specimens using a 3500-kN UTM. The test results indicate that the SPIP specimen has higher initial stiffness, peak stress, and strain ductility compared with others.

Keywords: Axial load, Circular spiral, Innovative confinement, Interlocking, Square spiral

1. INTRODUCTION

Reinforced concrete (RC) is a symbiotic mutualism of composite materials consisting of concrete and reinforcing steel materials [1-3]. Steel reinforcement in RC forms a reinforcement system consisting of longitudinal and transverse reinforcement. The longitudinal reinforcement configuration in a square reinforced concrete column (Square RCC) can be evenly distributed on each side or in the form of a bundling system. The transverse reinforcement can be in the form of stirrups tie or circular spiral as the traditional confinement is widely used so far [4,5] and has been accommodated in several codes [6].

Generally, the column cross-sections are square and circular [7], and many designers prefer square shapes because they are easier to manufacture, have a larger cross-sectional capacity. Although, in terms of aesthetics, circle forms are more attractive [8]. However, structural failure has an impact on the form of the column even though it has ductility. Failure at Square RCC was influenced by the reinforcement system factors, especially by the transverse reinforcement system.

Several researchers had conducted studies on the reinforcement system, especially in the transverse reinforcement as confinement to increase ductility, such as studying the effect of confinement due to different traditional confinement systems using a combination of hooks [9], confinement using multiple stirrups [10], utilize the type of hook with an interlocking system [11], utilize fine mesh as confinement [12], utilize circular spiral with an interlocking system [13], utilize welded wire mesh as confinement [14-19], combination of steel fiber and spiral [20,21], using a combination of a square spiral and an octagonal spiral that confined the concrete core [22], and even external confinement [23-25].

There has been no previous research on confinement using a square spiral with an interlocking system using a bundling system on longitudinal reinforcement. This research adheres to the concept - columns in columns - and this is the subject of this research.

This confinement system is in the column section's form to reduce the ineffective area of the concrete core. Its manufacture does not leave cuts as in conventional confinement manufacture, faster because the roll bar bender and assembling and installing it becomes easier in construction. It is more efficient in work and effective in its cross-sectional capacity.

The authors conducted a potential analysis of the existing confinement systems proposed by several previous researchers to obtain the subject of this research [26,27]. The analysis resulted in the proposed innovative confinement systems such as an interlocking square spiral confinement system with a circular spiral labeled SPIL, an octagonal spiral interlocking confinement system with a square spiral labeled SS8I, and an interlocking confinement system between square spiral with the SPIP label. To obtain performance data from each specimen using an innovative confinement system, the test method was carried out through an experimental approach in the laboratory using a compression machine with a capacity of 3500 kN to provide an axial load on each specimen. Each Square RCC test object's performance with the confinement system is shown through the stress-strain relationship pattern of the resulting data and comparing the benchmark specimen, namely the plain concrete column or Plain CC specimen.

2. MATERIALS AND METHOD

2.1 Materials

The material used in this study is a composite material as a structural material, namely concrete and steel reinforcement. The concrete materials used are following those specified in the code, such as cement using type 1 where for construction that does not require special requirements, the sand used passes through sieve No.4 and is stuck in sieve No. 100, the gravel used escapes the sieve No. 3/8 and stuck in sieve No. 8 [28]. The admixture used consists of two types, namely, types B and F [29]. Meanwhile, water as a mixture of these materials fulfills the general requirements, namely that it could be drunk and did not cause odor. The concrete was designed to have a strength (f'_c) 21 MPa at the age of 28 days, and this was following the minimum requirements specified in the code besides adjusting to the testing machine's capacity.

Another material used was steel reinforcement. Reinforcing steel was used for longitudinal and transverse reinforcement. Longitudinal reinforcement used reinforcement with strength (f_y) 427 MPa, for transverse reinforcement using steel reinforcement with strength (f_{yt}) 513 MPa. Both of them were types of deformed reinforcing steel and the strength used was the result of the tensile test.

2.2 Test setup and testing

The equipment used in this study consists of a pressure test machine with a capacity of 3500 kN as the main equipment and other supporting equipment in the form of a transducer which functions to send data information in the form of deformation of each load unit, a load cell which functions as a tool that accepts loads and is converted to compressive loads and a data logger which functions as a data recorder sent from the transducer and load cell through its sensors and computer devices that compile data records from the logger data in the form of load and deformation data output. The test setup and a photograph showing a UTM with a column specimen ready for testing are shown in Figs. 1 and 2.

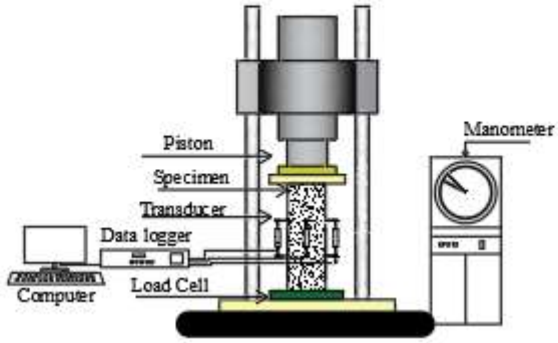

Fig. 1 Schematic test setup. Source: authors

Fig. 2 Photograph of UTM with a specimen ready for testing. Source: authors

2.3 Test specimens

To determine the performance of confined concrete and unconfined or plain concrete, it can be seen from the stress-strain relationship as shown in Fig. 3 [30]. Whereas the strain ductility is obtained by determining the Z value at the post-peak or descending branch as given by Eq. (1) [31]. The smaller the Z value, the more ductile the specimen is.

$$Z = \tan \Theta / f'_{pcc} \qquad (1)$$

where Θ is the angle formed between the peak stress (f'_{pcc}) and the stress after the peak stress when it drops to $0.5f'_{pcc}$ and between the corresponding strain at the peak stress (ε'_{pcc}) and the strain when the stress drops to $0.5f'_{pcc}$ ($\varepsilon'_{pcc0.5}$), respectively.

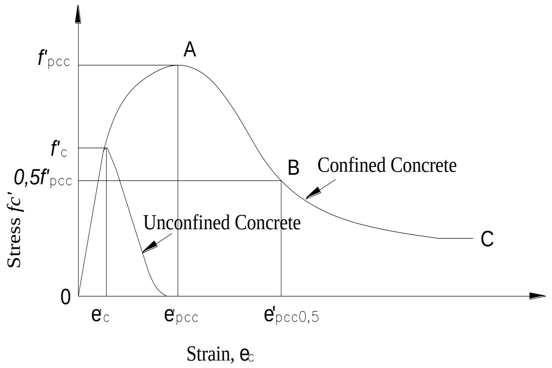

Fig. 3 Comparison of stress-strain relationships for unconfined concrete and confined reinforced concrete. Source: Paultre and Légeron (2008)

From the results of the potential analysis that had been done previously, the next step was to make the form and configuration of the reinforcement system consisting of a longitudinal and transverse reinforcement system, as shown in Fig. 4. Designing the factors and variables needed in this study to achieve research objectives such as determining the dimensions of the specimen with a size of 200 × 200 × 800 mm, the strength of steel reinforcement, and the compressive strength of the concrete according to the code requirements, the diameter of the longitudinal reinforcement was 13 mm with a total of 16 bars, the transverse reinforcement diameter was 6 mm and ensured a volumetric ratio of the transverse reinforcement of 1.51% for all confinement systems, determining this ratio to obtain fair reinforcement spacing for the three specimens. The specifications of the test specimens from the above research results were as shown in Table 1. Then made and assembled as in Fig. 5 and molded according to the predetermined dimensions. Prior to concreting, a concrete mix-design was carried out with a concrete compressive strength (f'_c) of 21 MPa using 10 mm screening crushed stone, admixture, and a water-cement value of 0.7 so that the slump value was controlled in the range of 180-190 mm and continued by conducting batch trials to ensure slump control and making cylindrical specimens for testing at the age of 28 days to get the strength as designed. After this stage, the concreting process was carried out for each test object, and the curing process was carried out for 28 days before laboratory testing was carried out. Before testing, a load cell installed, followed by setting up the specimen by installing a transducer on all four sides of the test region and connecting it to the data logger. The test was carried out by applying axial pressure until the specimen was crushed. The incoming data information was converted into a graphic by a computer device from the data logger.

Table 1 Details of specimens

Specimen ID	Dimension (mm)	Concrete Strength	Long. Steel	Trans. Steel				Vol. Ratio (%)
		f_c' (MPa)	Dia. (mm)	f_y (MPa)	Dia. (mm)	f_{yt} (MPa)	Spacing (mm)	
PC	200×200×800	21						
SPIL	200×200×800	21	13	427.37	6	513.28	133	1.514
SS8I	200×200v800	21	13	427.37	6	513.28	118	1.512
SPIP	200×200×800	21	13	427.37	6	513.28	152	1.515

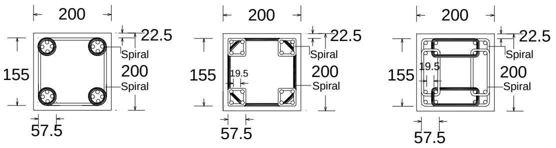

Fig. 4 Innovation confinement system form and configuration for (a) SPIL, (b) SS8I, and (c) SPIP specimens. Source: authors

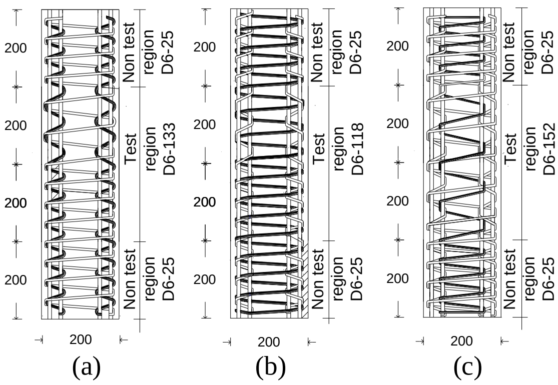

Fig. 5 Transverse reinforcement spacing and test and non-test region for (a) SPIL, (b) SS8I, and (c) SPIP specimens. Source: authors

3. RESULT AND DISCUSSION

3.1 Plain Concrete (PC) as Benchmark

The PC specimen's performance is shown in Fig. 6 in terms of stress-strain curve. Figure 7 shows when the specimen was subjected to axial load during testing. The stiffness of the ascending branch is around 20,133.12 MPa when the stress reaches $0.45f'_c$ as shown in Fig. 6 (Point a). In this condition, the PC specimen did not change shape as shown in Fig. 7(a). The maximum performance is achieved when the peak stress reaches 18.36 MPa when the strain is 0.00265 as shown in Fig. 6 (Point b). In this stage, the specimen was crushed at the support (Fig. 7(b)), and the stiffness decreased by 1,740.06 MPa.

The stiffness reduction continued after passing the peak stress until the specimen was crushed as shown in Figs. 6 (Point c) and Fig. 7(c). The strain ductility after the peak stress of this specimen ($0.8f'_{pc}$) is 1.521, and this proves that without any confinement system, the specimen could not develop strain ductility.

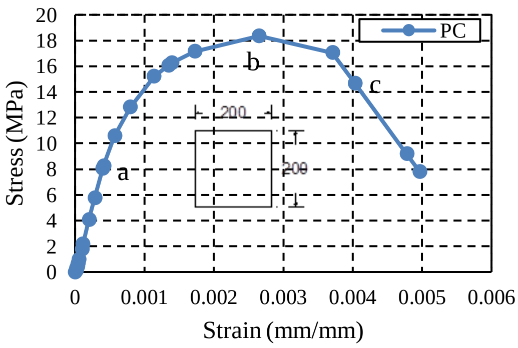

Fig. 6 Stress-strain curve of PC specimen. Source: authors

Fig. 7 Failure progress of PC specimen during testing. Source: authors

3.2 Square Spiral with Four Circular Spiral Interlocking Confinement System (SPIL)

The performance of SPIL specimen is described in terms of the stress-strain curve shown in Fig. 8. The progressive damage pattern of the specimen is given in Fig. 9. The initial specimen's secant stiffness at the stress of $0.45f'_{pcc}$ is about 25,648.36 MPa. At this stage, the specimen was still capable of maintaining its stable shape without any significant deformation as shown in Figs. 8 (Point a) and 9(a). The peak stress (f'_{pcc}) of about 31.76 MPa was achieved when the strain was around 0.00474 (Fig. 8 Point b). Some initial surface cracks of the cover began to occur at the top and bottom of the specimen as shown in Fig. 9(b). There were followed by the initial spalling of the cover. After the peak stress, the damages focused at the center height of the specimen which is the test region. The confining system of the SPIL specimen has increased the initial stiffness by about 27.57%, the peak stress by about 73.03%, and the strain at peak stress by about 78.8% compared to the corresponding values of the PC specimen. Meanwhile, the strain ductility of the specimen which is taken when the stress drops to $0.8f'_{pcc}$ is about 3.98. This showed that the reinforcement system and the SPIL configuration has increased the strain ductility of 161.32% higher than the that of the PC specimen.

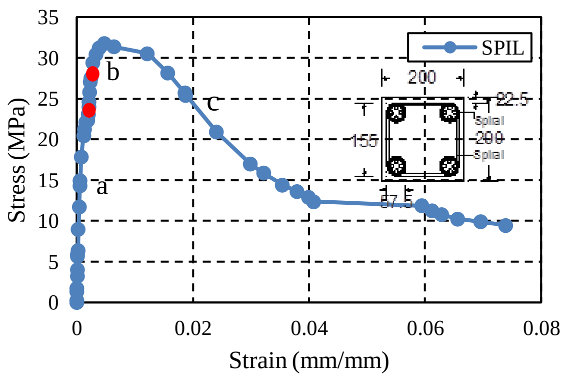

Fig.8. Stress-strain curve of SPIL specimen. Source: authors

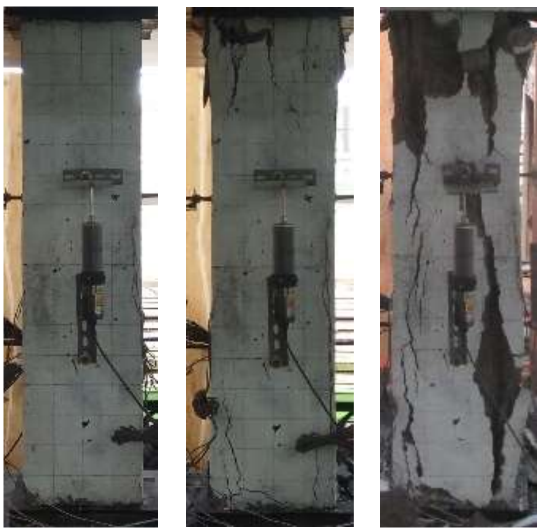

Fig. 9 Failure progress of SPIL specimen during testing. Source: authors.

3.3 Octagonal Spiral with Four Square Spiral Interlocking Confinement System (SS8I)

The stress-strain curve of SS8I specimen in Fig. 10 (Point a) shows that the specimen's initial stiffness at $0.45f'_{pcc}$ is approximately 26,967.78 MPa. At this stage, the specimen did not undergo any significant deformation changes as shown in Fig. 11(a). The peak stress (f'_{pcc}) of around 32.89 MPa was achieved when the strain was about 0.00297 as shown in Fig. 10 (Point b). In this condition, the specimen started to crack at the surface of concrete cover as shown in Fig. 11(b). Significant damage began to occur on the specimen beyond the peak stress. The specimen was damaged mainly in the test region as expected in the form of large deformation primarily in the lateral direction. By providing the SS8I confining system in the specimen, it has increased the initial stiffness by about 33.95%, the peak stress by about 79.14%, and the strain at the peak stress by about 12.12% compared to the corresponding values of the PC specimen. The strain ductility of the specimen which is taken when the stress drops to $0.8f'_{pcc}$ is about 9.33. This showed that the reinforcement system and the SPIL configuration has increased the strain ductility of 513.31% higher than the that of the PC specimen.

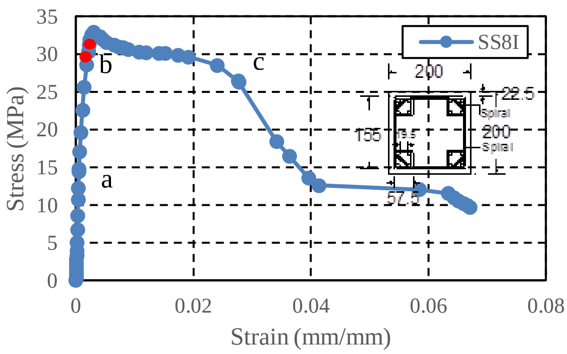

Fig. 10 Stress-strain curve of SS8I specimen. Source: authors

(a) (b) (c)

Fig. 11 Failure progress of SS8I specimen during testing. Source: authors

3.4 Interlocking Confinement System between Square Spiral (SPIP)

From Fig. 13(a), it can be seen that the SPIP specimen under initial loading up to $0.45f'_{pcc}$ did not experience significant deformation changes, and the corresponding stiffness of the specimen is about 26,971.39 MPa. The peak stress (f'_{pcc}) of about 34.54 MPa was attained when the strain was around 0.00319 as shown in Fig. 12 (Point b). At this level, the indication of initial concrete spalling began to appear where cracks progressively occurred in the test region as shown in Fig. 13(b). Significant damages of the specimen start to occur after the post-peak of the curve as shown in Fig. 12 (Point c) where the tangible deformation changes of the specimen began with the oblique cracks occurred severely in the test region. At this stage, spalling of the cover started to occur mainly in the mid-height region of the specimen as as shown in Fig. 13(c).

By providing the SPIP confining system in the specimen, it has increased the initial stiffness by about 33.97%, the peak stress by about 88.19%, and the strain at the peak stress by about 20.29% compared to the corresponding values of the PC specimen. The strain ductility of the specimen which is taken when the stress drops to $0.8f'_{pcc}$ is about 7.85. This showed that the reinforcement system and the SPIL configuration has increased the strain ductility of 415.80% higher than the that of the PC specimen.

When the specimens reached their final failures (the strength dropped to about $0.15f'_{pcc}$'), they had very long strains with mostly constant strengths up to around 0.07 of strain before the tests were terminated afterwards. This is one of the advantages by introducing the confinement system in reinforced concrete columns.

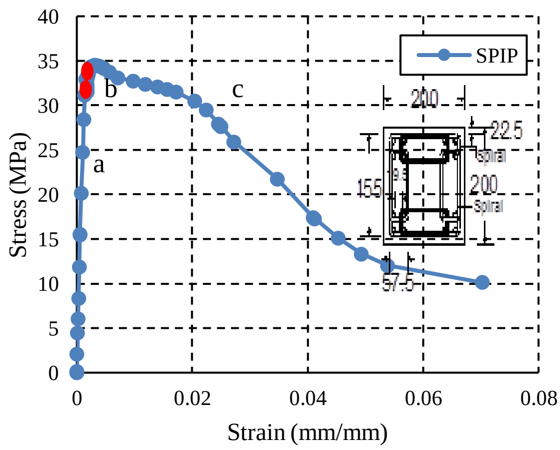

Fig. 12 Stress-strain curve of SPIP specimen. Source: authors

(a) (b) (c)

Fig. 13 Failure progress of SPIP specimen during testing. Source: authors

3.5 Comparison of Performances of Each Confinement System

The performance of each specimen, as in Fig. 14 and Table 2, shows that the SPIP specimen has the initial stiffness of 0.1% and 5.01% higher than those of the SS8I and SPIL specimens, respectively. In terms of peak stress (f'_{pcc}), the SPIP specimen had the strength of 5.01% and 8.75% higher than those of the SS8I and SPIL specimens, respectively. Meanwhile, in terms of strain ductility after peak stress, the SS8I specimen had the strain ductility of about 18.90% and 135.69% higher than those of the SPIP and SPIL specimens, respectively. For the initial strain up to the peak stress, the SPIL specimen has strain of about 48.86% and 59.60% longer than those of the SPIP and SS8I specimens, respectively. SS8I specimen had the strength and strain ductility of 3.56% and 135.69% higher than that of the SPIL specimen. The SS8I specimen also had an initial strain of about 18.90% higher than that of the SPIP specimen.

Table 2 Test result parameters of specimens

Specimen ID	Initial Stiffness (MPa)		Initial Strain (ε_i)		Stress (f'_{pcc}) (MPa)		Strain Ductility (μ_ε)	
PC	20,133.12	1.000	0.00265	1.000	18.36	1.000	1.521	1.000
SPIL	25,684.36	1.276	0.00474	1.788	31.76	1.730	3.959	2.613
SS8I	26,967.78	1,339	0.00297	1.121	32.89	1.791	9.331	6.133
SPIP	26,971.39	1.340	0.00319	1,204	34.54	1.881	7.848	5.158

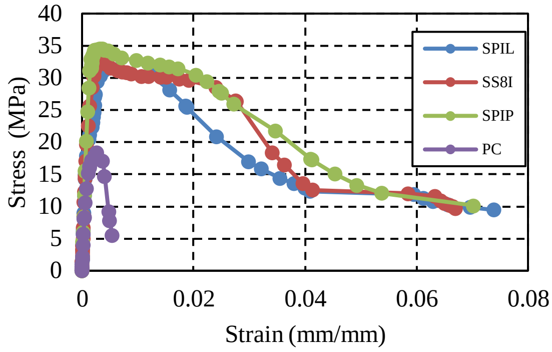

Fig. 14 Comparison of stress-strain curves of four test specimens. Source: authors.

4. CONCLUSION

From the data and analysis of each specimen above, it can be concluded as follows:

1. The SPIP confinement system performed the best in improving the column's initial stiffness, strength, and strain ductility compared to the other confinement systems.
2. The SPIL confinement system provided the best contribution in increasing the column initial strain before the maximum load compared to the other confinement systems.
3. The SPIP specimen had the highest initial stiffness, strength, and strain ductility after peak stress than the other specimens.
4. The SPIL specimen had the longest strain than the other specimens.
5. The interlocking confining system that intersects bundles of reinforcement and surrounds the concrete core in addition to the main spiral of the SPIP specimen provides additional stiffness and strength to the square column. It does not allow for an arching effect to occur in concrete core.
6. The circular spiral of the SPIL specimen could not effectively contribute to the strength of the square column due to the less inertia effect than the square spiral and the arching effect on the main confinement. However, this confining system provides greater initial strain prior to the peak stress compared to the other confinement systems.
7. The octagonal spiral of the SS8I specimen could not effectively contribute to the initial stiffness due to the less inertia effect than the square spiral and the arching effect on the main confinement. However, this confining system improved the strength better compared to the circular spiral.

5. ACKNOWLEDGMENTS

The authors would like to express their sincere gratitude to the General Director of Higher Education, Ministry of Education and Culture of Indonesia for the research grant received and the Center of Research and Development of Human Settlement, the Ministry of Public Works and Public Housing of Indonesia for providing the laboratory testing facility to make this research possible, and the Institute for Research and Community Service, Universitas Wijaya Kusuma Surabaya, which had facilitated the research grant process.

6. REFERENCES

[1] Wang C.K.; Salmon C.G. and Pincheira J.A., Reinforced Concrete Design, John Wiley & Sons, Inc., New York, 2007, pp. 1-3.

[2] Raka IG.P.; Tavio and Astawa, M.D., State-of-the-Art Report on Partially-Prestressed Concrete Earthquake-Resistant Building Structures for Highly-Seismic Region, Procedia Eng. J., Elsevier, Vol. 95, 2014, pp. 43-53.

[3] Wahjudi D.I.; Sugihardjo H. and Tavio, Behavior of Precast Concrete Beam-to-Column Connection with U- and L-Bent Bar Anchorages Placed Outside the Column Panel–Experimental Study, Procedia Eng. J., Elsevier, Vol. 95, 2014, pp. 122-131.

[4] El-Kholy A.M. and Dahish H.A., Improved Confinement of Reinforced Concrete, Ain Shams Eng. J., Vol. 7, No. 2, 2016, pp. 717-728.

[5] Agustiar; Tavio; Raka IG.P. and Anggraini R., Behavior of Concrete Columns Reinforced and Confined by High-Strength Steel Bars, Int. J. Civ. Eng. Tech., IAEME, Vol. 9, No. 7, 2018, pp. 1249-1257.

[6] ACI Committee 318, Building Code Requirements for Structural Concrete (ACI318-19) and Commentary on Building Code Requirements for Structural Concrete (ACI 318R-19), Farmington Hills, American Concrete Institute, 2019.

[7] Flanella D.A., Reinforced Concrete Structure, McGraw Hill, New York, 2011, pp. 407-408.

[8] Subramanian N., Design of Reinforced Concrete Structures, Oxford University Press, New Delhi, 2013, pp. 46-47.

[9] Lau W.C., Strength of Axially Loaded Reinforced Concrete Columns, B.Eng. Thesis, Dept. Civ. Struct. Eng., The Hong Kong Polytechnic, 1999.

[10] Chan K.M., Ultimate Strength of Reinforced Concrete Column with Different Arrangement of Links, B.Eng. Thesis, Dept. Civ. Struct. Eng., The Hong Kong Polytechnic, 2001.

[11] Chung W.M. and Lam E.S., Confinement Action of Reinforced Concrete Columns with Non-Seismic Detailing, 4th Int. Conf. Earthquake Eng., Paper No. 304, Taipei, 2006, pp. 1-9.

[12] Tavio; Purwono R. and Ashari M.L., Confinement of Circular RC Columns with Fine Mesh, Int. Conf. Earthquake Eng. Disaster Mitigations, Jakarta, 2008, pp. 502-509.

[13] Yin S.L.; Wu T.L.; Liu T.C.; Sheikh S.A. and Wang R., Interlocking Spiral Confinement for Rectangular Columns, Concrete Int., American Concrete Institute, Vol. 33, No. 12, 2011, pp. 38-45.

[14] Tavio and Kusuma, B., Ductility of Confined Reinforced Concrete Columns with Welded Reinforcement Grids, Excellence in Concrete Construction through Innovation–Proc. Int. Conf. Conc. Const., CRC Press, Taylor and Francis Group, 2009, pp. 339-344.

[15] Tavio and Kusuma B., Experimental Behavior of Concrete Columns Confined by Welded Wire Fabric as Transverse Reinforcement under Axial Compression, ACI Struct. J., American Concrete Institute, Vol. 109, No. 3, 2012, pp. 339-348.

[16] Kusuma B. and Tavio, Axial Load Behavior of Concrete Columns with Welded Wire Fabrics as Transverse Reinforcement, Procedia Eng. J., Elsevier, Vol. 14, 2011, pp. 2039-2047.

[17] Tavio and Kusuma B., Investigation of Stress-Strain Models for Confinement of Concrete by Welded Wire Fabric, Procedia Eng, J., Elsevier, Vol. 14, 2011, pp. 2031-2038.

[18] Tavio and Kusuma B., Stress-Strain Model for High-Strength Concrete Confined by Welded Wire Fabric, Disc., J. Mat. Civ. Eng., American Society of Civil Engineers, Vol. 21, No. 1, 2009, pp. 40-45.

[19] Tavio and Kusuma B., Strength and Ductility Enhancement of Reinforced HSC Columns Confined with High-Strength Transverse Steel, Proc. Eleventh East Asia-Pacific Conf. Struct. Eng. Const., 2008, pp. 350-351.

[20] Sabariman B.; Soehardjono A.; Wisnumurti; Wibowo A. and Tavio, Stress-Strain Behavior of Steel Fiber-Reinforced Concrete Cylinders Spirally Confined with Steel Bars, Adv. Civ. Eng., Hindawi, Vol. 2018, 6940532, 2018, pp. 1-8.

[21] Sabariman B.; Soehardjono A.; Wisnumurti; Wibowo A. and Tavio, Stress-Strain Model for Confined Fiber-Reinforced Concrete under Axial Compression, Archives of Civil Engineering, Polish Academy of Sciences, Vol. 66, No. 2, 2020, pp. 119-133.

[22] Kim, H.G.; Jeong C.Y.; Kim D.H. and Kim K.H., Confinement Effect of Reinforced Concrete Columns with Rectangular and

Octagon-Shaped Spirals, MDPI J., 2020, pp. 1-10.

[23] Pudjisuryadi P. and Tavio, Axial Compressive Behavior of Square Concrete Columns Externally Collared by Light Structural Steel Angle Sections, Int. J. Appl. Eng. Res., Research India Publications, Vol. 11, No. 7, 2016, pp. 4655-4666.

[24] Pudjisuryadi P. and Tavio, Performance of Square Reinforced Concrete Columns Externally Confined by Steel Angle Collars under Combined Axial and Lateral Load, Procedia Eng. J., Elsevier, Vol. 125, 2015, pp. 1043-1049.

[25] Pinto D.; Tavio and Raka IG.P., Axial Compressive Behavior of Square Concrete Columns Retrofitted with GFRP Straps, Int. J. Civ. Eng. Tech., IAEME, Vol. 10, No. 1, 2019, pp. 2388-2400.

[26] Machmoed S.P.; Tavio and Raka IG.P., A Proposed Innovative Confinement of Square Reinforced Concrete Columns for Ductility Improvement, SSRN, Elsevier, 2020, 3512742, pp. 1-10.

[27] Machmoed S.P.; Tavio and Raka IG.P., Potential of New Innovative Confinement for Square Reinforced Concrete Columns, J. Phys.: Conf. Ser., IOP, Vol. 1469, 012027, 2020, pp. 1-7.

[28] ASTM International, Annual Book of ASTM Standards, West Conshohocken, ASTM International, Vol. 04.01, 2003.

[29] ASTM International, Annual Book of ASTM Standards, West Conshohocken, ASTM International, Vol. 04.02, 2003.

[30] Paultre P. and Légeron F., Confinement Reinforcement Design for Reinforced Concrete Columns, J. Struct. Eng., ASCE, Vol. 134, No. 5, 2008, pp. 738-749.

[31] Park R. and Paulay T, Reinforced Concrete Structures. John Willey and Sons, Toronto, Canada, 1975, pp. 21-28.